

Dimethyl 2,5-furandicarboxylate synthesis from 2,5-furanodicarboxylic acid and dimethyl carbonate in presence of MgO-Al₂O₃ and tetrabutylammonium bromide

Chunyu Meng, Kunmei Su^{*}, Zhenhuan Li^{*}, Maliang Zhang

Tianjin Key Laboratory of Green Chemical Technology and Process Engineering, School of chemistry and chemical engineering, Tiangong University, No. 399 Binshui West Street, Tianjin 300380, PR China

ARTICLE INFO

Keywords:

2,5-Furanodicarboxylic acid
Esterification
Dimethyl 2,5-furanedicarboxylate
Dimethyl carbonate
Acid base synergistic catalysis

ABSTRACT

2,5-furandicarboxylic acid (FDCA) and dimethyl 2,5-furandicarboxylate (DMFDCA) are attracting increasing attention as important biomass-based chemical feedstocks. Considering the physicochemical properties of FDCA with high polarity, poor solubility and easy decarboxylation, the synthesis of DMFDCA from FDCA is especially necessary. However, how to synthesize DMFDCA in case of avoiding a series of side reactions such as furan ring opening and double bond addition is a huge challenge. Herein, we used FDCA and dimethyl carbonate (DMC) to synthesize DMFDCA in presence of MgO-Al₂O₃ and tetrabutylammonium bromide (TBAB), and the optimized yield and selectivity of DMFDCA came up to 76.38% and 80.19%, respectively. In addition, the used catalysts were characterized by SEM, XRD, BET, XPS and CO₂-TPD analysis, and the structure, composition, morphology and basic site distribution of catalyst were well studied, and the relationship between catalyst structure and catalytic performance in the esterification of FDCA into DMFDCA through organic acid exchange reaction method was also analyzed. This work provides a promising solution for the preparation of furan-based polyester monomers.

1. Introduction

Polyester materials play an important role in modern life [1], unfortunately, most polyester monomers are derived from fossil fuels [2], which increases the depletion of fossil and results in environmental pollution [3]. Therefore, it is of great significance to find some bio based polyester monomers to replace traditional fossil resource monomers.

FDCA is a product obtained by the selective oxidation of 5-hydroxymethyl furfural (HMF) [4-6]. The most important application of FDCA is to polymerize with ethylene glycol (EG) to produce polyethylene 2,5-furandicarboxylate (PEF) instead of petroleum based polyester polyethylene terephthalate (PTA) [7]. Although the high yield of FDCA can be obtained by the oxidation of HMF, the physicochemical properties of FDCA become a bottleneck for its further application, for example, high polarity, big boiling point, easy decarboxylation and poor solubility [8]. However, DMFDCA, as the ester product of FDCA, not only has a low boiling point but also has the excellence solubility in most common solvents. Most importantly, it can avoid the

decarboxylation of FDCA at high temperature [9]. These advantages will benefit the potential applications of DMFDCA in materials, energy and chemical industries.

According to the previous literature, DMFDCA can be prepared from HMF. Recently, it was reported that 92.00% yield of DMFDCA could be obtained from HMF and methanol by Au-Fe₃O₄ NPs catalytic oxidation in presence of O₂ [10], however, the precious metals are needed as catalysts to obtain the high yields of DMFDCA. Another research group [11] reported that DMFDCA could be synthesized from FDCA and methanol in the presence of strong inorganic acid (H₂SO₄, 80 °C, 12 h), while the yield of DMFDCA was low. Most importantly, the addition of strong inorganic acids to the reaction system will lead to the formation of furan rings as a side reaction, resulting in a lower selectivity [12]. Therefore, it is of great significance to develop a green and efficient method for DMFDCA synthesis.

Dimethyl carbonate (DMC) has been of great interest as a good alternative to highly toxic reagents such as dimethyl sulfate and phosgene (COCl₂) [13-15], due to the non-toxicity and high active sites [16, 17]. In addition, DMC is a good methylation reagent, especially it is

^{*} Corresponding authors.

E-mail addresses: sukunmei@tiangong.edu.cn (K. Su), lizhenhuan@tiangong.edu.cn (Z. Li).

<https://doi.org/10.1016/j.mcat.2021.111707>

Received 6 April 2021; Received in revised form 21 May 2021; Accepted 7 June 2021

Available online 20 June 2021

2468-8231/© 2021 Elsevier B.V. All rights reserved.

suitable for water sensitive alkylation [18, 19]. If DMC acts as the methylating reagent, the byproduct is CO₂ and methanol, and methanol in turn can be synthesized into DMC [20].

Herein, we report a highly efficient method for the synthesis of DMFDCA from FDCA and DMC using bimetallic oxide/TBAB as catalyst, and the effects of MgO catalysts on the reaction selectivity were studied. The catalysts were well characterized by X-ray diffraction (XRD), scanning electron microscopy (SEM), N₂ adsorption (BET), X-ray photoelectron spectroscopy (XPS) and temperature programmed desorption of carbon dioxide (CO₂-TPD), and the reaction mechanism between DMC and FDCA was also studied. The large-scale synthesis of DMFDCA from DMC and FDCA is expected to be achieved in this reaction system with the high efficiency, selectivity and mild conditions.

2. Experimental section

2.1. Catalyst preparation

MgO-Al₂O₃ and MgO-La₂O₃ were prepared by the hydrothermal method. Firstly, MgO-Al₂O₃ was prepared from 15 mmol magnesium nitrate hexahydrate and 5 mmol aluminum nitrate which were dissolved in 75 mL deionized water and stirred until completely dissolved. Subsequently, 75 mL urea solution was dropped into the above solution and stirred for 1 h to obtain a clear solution. Then, the mixed solution was transferred into a stainless steel autoclave which was lined with Teflon. After being treated at 160 °C for 12 h, the obtained precipitate was washed with distilled water to neutrality and dried at 60 °C for 12 h. The obtained precursor was calcined in air at different temperatures (450 °C, 550 °C, 650 °C) for 4 hour, thus, the MgO-Al₂O₃ was prepared. The preparation process of MgO-La₂O₃ was the similar with the above method, and the molar ratio of La to Mg is 1:3, and obtained MgO-La₂O₃ precursor was calcined in air at different temperatures (650 °C, 750 °C, 850 °C) to obtain the different catalysts.

2.2. Catalysts characterization

The X-ray diffraction (XRD) pattern was carried out on a Bruker D8 Advance X-ray diffractometer equipped with a monochromatic detector and equipped with CuK α radiation with a wavelength of 0.154 nm. The scanning angle is 2 θ –80°, the scanning rate is 5°/min, the working current is 40 mA, and the voltage is 40 kV. X-ray photoelectron spectroscopy (XPS) was performed by THERMO ESCALAB 250XZ. The binding energy (Eb) is internally calibrated by the binding energy of carbon deposit C1 at 284.6 eV. The N₂ adsorption desorption curves of the prepared catalysts were measured by quantachrome autosorb-iq-2mp apparatus from quantachrome company. The Brunauer Emmett teller method (BET) with desorption branches was used to calculate the specific surface area and pore size, respectively. The distribution of basic sites of the samples was determined by temperature programmed desorption (TPD) using chembet TPR/TPD under He gas atmosphere. The sample (50 mg) was exposed to He gas flow. The temperature was increased from room temperature to 750 °C at a rate of 10 °C/min. Scanning electron microscopy (SEM) images were measured by a Zeiss instrument, and the accelerating voltage of the instrument was 10 kV.

2.3. Esterification reaction of FDCA with DMC

The reaction was carried out in a three-necked flask. In a typical experiment, 6 mmol FDCA, 90 mmol DMC, 1.8 mmol TBAB were dissolved in 15 mL DMF, and the reaction was catalyzed by 0.6 mmol catalyst, and reaction temperature and reaction time were 150 °C, 6 h, respectively. After reaction, the yield of product was determined by HPLC. Methanol and water were used as mobile phase (V/V = 50:50) at a flow rate of 1.0 mL/min. The FDCA and DMFDCA retention times were 1.2 and 4.0 min, respectively.

3. Results and discussion

3.1. Effect of reaction conditions on methyl esterification

3.1.1. Effect of reaction temperature and reaction time

As shown in Fig. 1, the effects of different reaction conditions on FDCA conversion and DMFDCA yield was discussed. Reaction temperature is an important factor affecting FDCA methylesterification. The effect of reaction temperature on the catalytic reaction is shown in Fig. 1a. The yield of DMFDCA was 28.18% when the reaction temperature was lower ($T = 120$ °C). When the reaction temperature was increased ($T = 150$ °C), the yield of DMFDCA was 66.68%. A higher reaction temperature facilitates the endothermic reaction to proceed, and increasing the reaction temperature facilitates the solubility of FDCA in organic systems, which allows sufficient contact between reactants. When the temperature exceeded 150 °C, the increase of DMFDCA yield was no longer significant. This is mainly due to the high temperature will lead to a large number of DMC volatilization, which has a negative impact on the reaction. Therefore, the optimal reaction temperature should be at 150 °C.

The reaction time is also an important factor affecting the FDCA methylesterification reaction. In this experiment, the variation of the reaction time ranged from 2 to 10 h, and the DMFDCA yield is shown in Fig. 1b. In the first 2 h of the reaction, the conversion of FDCA reached a high level, but the yield of DMFDCA was surprisingly low, which may be due to FDCA raw materials are more easily converted into intermediate products and the slow reaction speed of DMC, resulting in the low yield of DMFDCA. When the reaction time was more than 4 h, the yield of DMFDCA increased rapidly. When the reaction time was 6 h, the highest yield was 66.68%. When the reaction time was more than 6 h, the yield of DMFDCA decreased slightly. Therefore, the optimal reaction time is 6 h.

3.1.2. Effect of catalyst ratio on esterification

Effect of the ratio of catalysts on the yield of DMFDCA is shown in Table 1. The reaction temperature was 150 °C for 6 h at a fixed molar ratio of FDCA to DMC of 1:15. As can be seen by entries 1 and 2, the yield of DMFDCA was lower in the reaction system lacking both MgO and TBAB. Either too much or too little MgO was unfavorable for the reaction to proceed (entries 3–8). Too much MgO might hinder the heat transfer from the oil bath to the reaction mixture, meanwhile, and too little MgO could not provide enough active sites for the reaction. TBAB as a phase transfer catalyst (PTC) was able to increase the solubility of MgO in the organic reaction system, and it can be seen by comparing different concentrations of TBAB (entry 6, entries 9–11) that an excess of TBAB was not conducive to the improvement of the DMFDCA yield. An excess amount of catalyst would make the reaction system viscous and disfavor the contact between reactants. Therefore, the optimal catalyst ratio for methyl esterification reaction is 1:0.1:0.3.

3.2. MgO-Al₂O₃ catalyzed FDCA methyl esterification

To examine the effect of base sites distribution on the reaction of FDCA with DMC, MgO-Al₂O₃ and MgO-La₂O₃ were used as catalysts to catalyze the reaction between FDCA and DMC under the optimum reaction conditions, respectively. Furthermore, the structures of MgO-Al₂O₃ and MgO-La₂O₃ were well characterized.

In order to determine the crystal structure of the catalysts obtained at different temperatures, XRD patterns of Mg-Al compounds were shown in Fig. 2a. For Mg-Al compounds obtained at 450 °C, the XRD peaks mainly appeared at 32.6°, 35.8°, 42.9°, 46.8° and 53.8°, which were corresponded to the crystal planes (104), (006), (113), (202), (018). And after comparison with the standard card (JCPDS 78–2442), it was found that the obtained substance was MgCO₃ [21]. As for the substances obtained at 550 °C and 650 °C, the XRD peaks appeared at 36.8°, 42.8°, 62.1°, 74.5° and 78.4°, which were corresponded to the crystal planes of

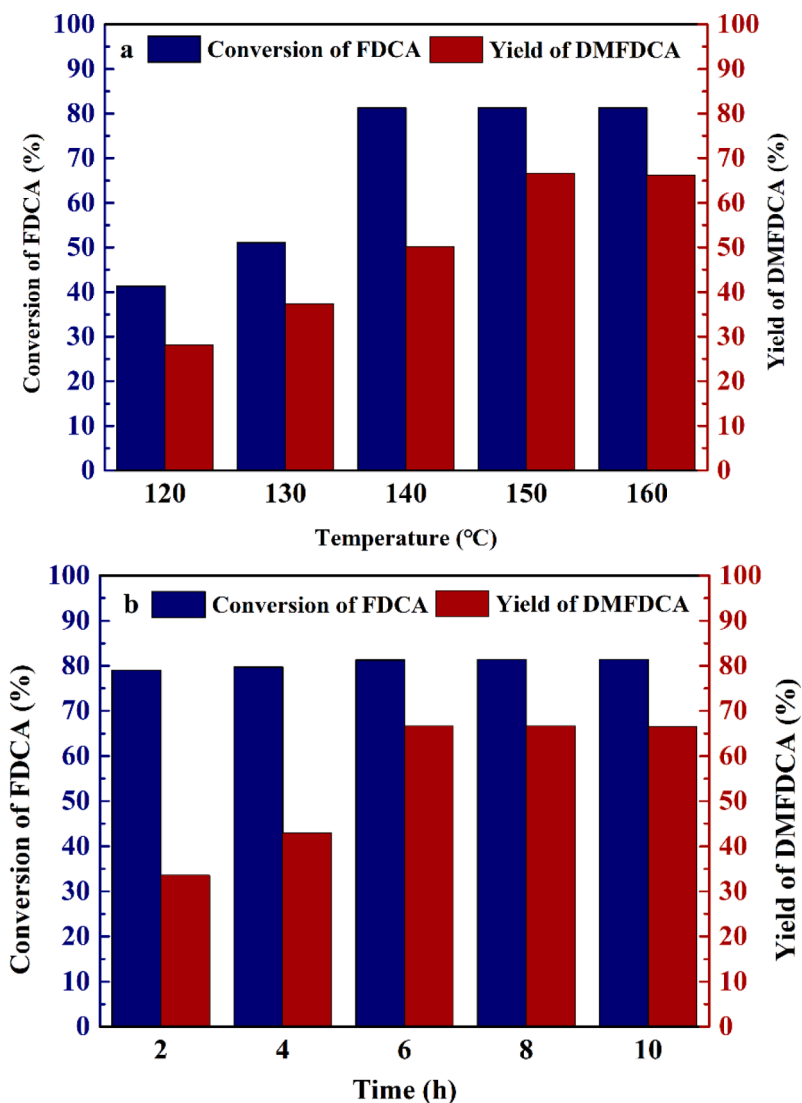


Fig. 1. Effects of reaction temperature (a) and reaction time (b) over MgO.

Table 1

The influence of the ratio of FDCA, MgO and TBAB on the esterification.

Entry	FDCA:MgO:TBAB	Conversion of FDCA(%)	Yield of DMFDCA(%)
1	1: 0:0.3	26.00	23.00
2	1: 0.3 :0	22.16	19.13
3	1: 1.5 :0.3	61.34	58.07
4	1: 1:0.3	67.28	64.07
5	1: 0.5 :0.3	70.60	66.65
6	1: 0.1 :0.3	81.29	66.68
7	1: 0.05 :0.3	71.45	58.99
8	1: 0.01:0.3	58.26	55.50
9	1: 0.1:0.6	69.10	55.73
10	1:0.1:0.9	78.09	62.25
11	1:0.1:0.15	66.03	54.63

Reaction conditions: solvent (DMF), atmospheric pressure, stirring speed 400 rpm.

(111), (200), (220), (311), (222). These could be attributed to the MgO by comparison with standard cards (JCPDS 75–0447) [22]. Moreover, the XRD peak of MgO obtained at 550 °C was broad and weak, and the intensive peak of MgO obtained at 650 °C indicated that the catalysts had a better crystal structure. In order to determine the structure of Al atom in catalyst, the binding energy of Al and O elements was analyzed by XPS (As shown in Fig. 2c and d). From XPS analysis of Al 2P and O 1S

in the catalyst calcinated at 450 °C, it was found that Al species was mainly in Al(OH)₃ formation, while Al₂O₃ was obtained at 550 °C and 650 °C [23]. The characteristic diffraction peaks of Al₂O₃ were not found in XRD, which indicated that Al₂O₃ was well dispersed or presented with an amorphous structure. Fig. 2b shows the effect of using MgCO₃-Al(OH)₃ and MgO-Al₂O₃ as catalysts on the methyl esterification reaction of FDCA, respectively. In the MgCO₃-Al(OH)₃ involved FDCA methylation reaction, the conversion of FDCA was 91.60%, and the yield of DMFDCA was 57.57%. In the MgO-Al₂O₃ catalyzed methyl esterification of FDCA, the conversion of FDCA was 95.24%, and the yield of DMFDCA was 76.38%. In the system with MgCO₃-Al(OH)₃ as catalyst, the catalytic effect is poor because MgCO₃ is unstable at high temperature and Al(OH)₃ can not provide sufficient basic sites for the esterification of FDCA. And the Mg-O with medium basic strength is more favorable of transesterification.

The XRD analysis of MgO-Al₂O₃ before and after the catalytic reaction was shown in Fig. 3a. It could be seen that MgO-Al₂O₃ maintained a good crystal structure without new crystalline phase generation after reaction. However, compared with the fresh catalyst, the crystal surface exposure of recycled catalyst decreased slightly, which may be the reason for the decrease of catalytic activate. The cycling stability of the catalysts was shown in Fig. 3b, it still maintained a relatively good catalytic effect after 8 cycle catalysis. The conversion of FDCA was

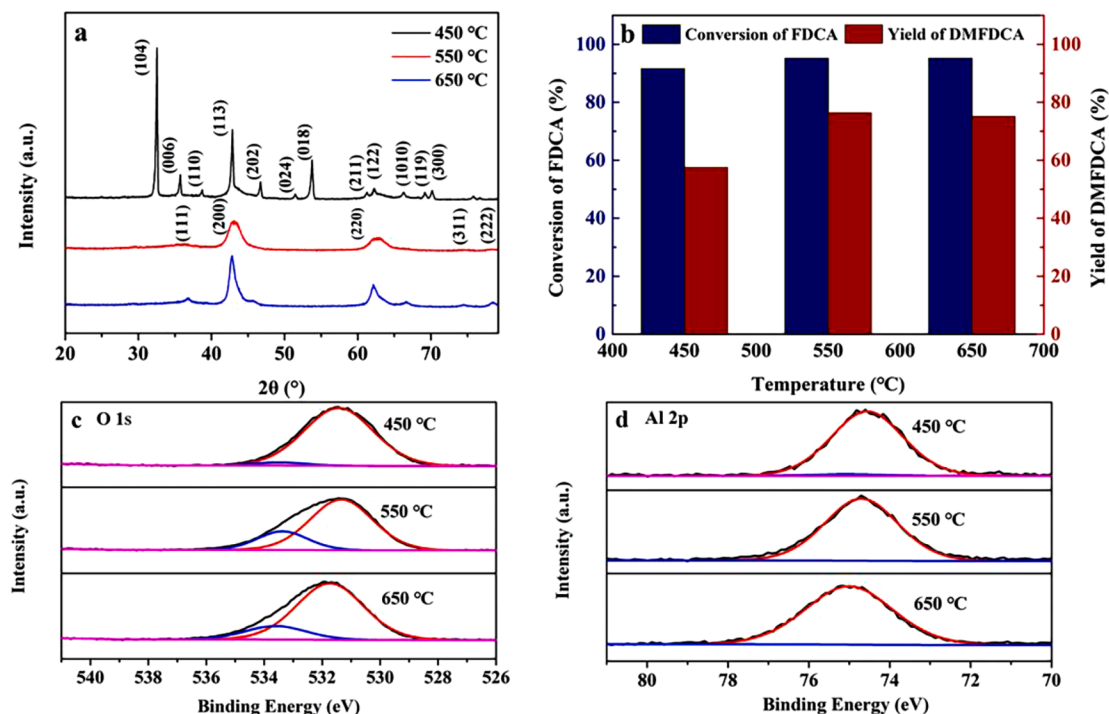


Fig. 2. XRD patterns of (a) Mg-Al compounds, (b) Conversion and yield, (c) XPS of O 1 s, and (d) Al 2p.

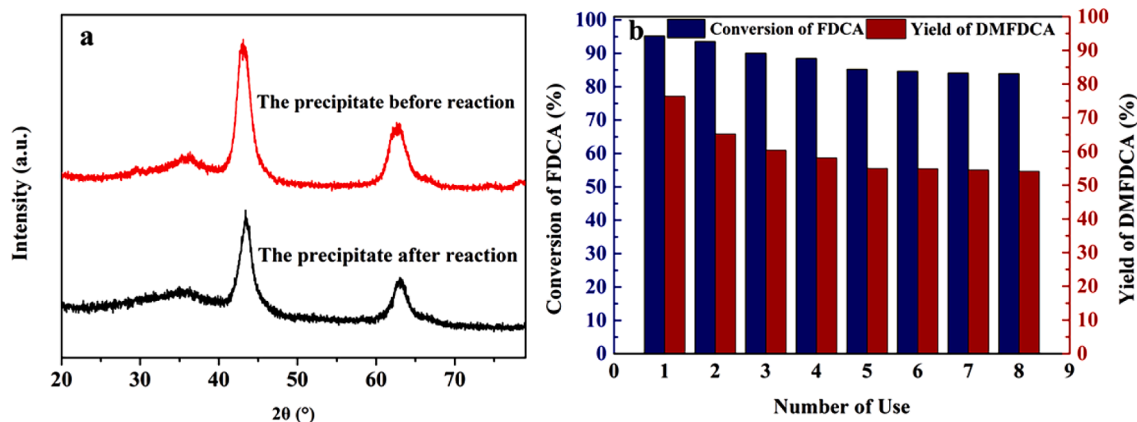


Fig. 3. XRD patterns of MgO-Al₂O₃ before and after reaction (a), and the cycle stability of the catalyst (b).

85.20%, and the yield of DMFDCA was 55.03%.

Fig. 4 shows the N₂ adsorption / desorption isotherm curve of MgO-Al₂O₃. It can be seen that the catalyst belongs to type IV isotherm, and the H₂ hysteresis curve appears in the range of 0.65–1.0 of high specific pressure (P/P₀). The specific surface areas of the catalysts before and after the reaction were 136 m²/g and 54 m²/g, respectively. It can be seen that the specific surface area of fresh catalyst and regenerated catalyst has a great influence on the reaction. However, the pore size of the catalysts did not change significantly, which was due to the presence of MgO-Al₂O₃ in the form of multilayered stacks (As shown in Fig. 5). The sheet structure of MgO-Al₂O₃ provides ample reactive sites for reactants, which also benefit to the desorption of reactants and products after the reaction. The pore size of the catalyst was not the main factor affecting the cycle stability of the catalyst.

3.3. MgO-La₂O₃ catalyzed FDCA methyl esterification

Fig. 6a is the XRD diffraction pattern of Mg-La compounds after

calcination at three temperatures. No La₂O₃ was found at 650 °C, the XRD peaks appeared at 22.3°, 25.2°, 27.6°, 30.4°, 33.7°, 42.5°, 44.4°, 47.4°, 50.2°, 53.1° and 56.9°, could be indexed to (004), (100), (101), (102), (103), (006), (106), (110), (107), (114), (203) and (116) lattice planes of the La₂O₂CO₃ (JCPDS 84–1963) [24]. The characteristic peaks of La₂O₃ appeared in 26.0°, 29.1°, 29.9°, 39.4°, 46.0°, 52.1°, 55.3°, 55.8° and 62.2° matched with (100), (002), (011), (012), (110), (103), (112), (201) and (202) crystallographic planes of the hexagonal La₂O₃ (JCPDS 73–2141) [25]. Fig. 6b shows the effect of using MgO-La₂O₂CO₃ and MgO-La₂O₃ as catalysts on the methyl esterification reaction of FDCA, respectively. When MgO-La₂O₂CO₃ was involved in the esterification of FDCA, the conversion of FDCA was 88.52%, and the yield of DMFDCA was 57.38%. When MgO-La₂O₃ (calcination temperature=750 °C) participated in the esterification of FDCA, the conversion of FDCA was 88.57%, and the yield of DMFDCA was 69.77%. When MgO-La₂O₃ (calcination temperature= 850 °C) participated in the esterification of FDCA, the conversion of FDCA was 80.12%, and the yield of DMFDCA was 50.69%. The obtained MgO-La₂O₃ at 750 °C and 850 °C showed a

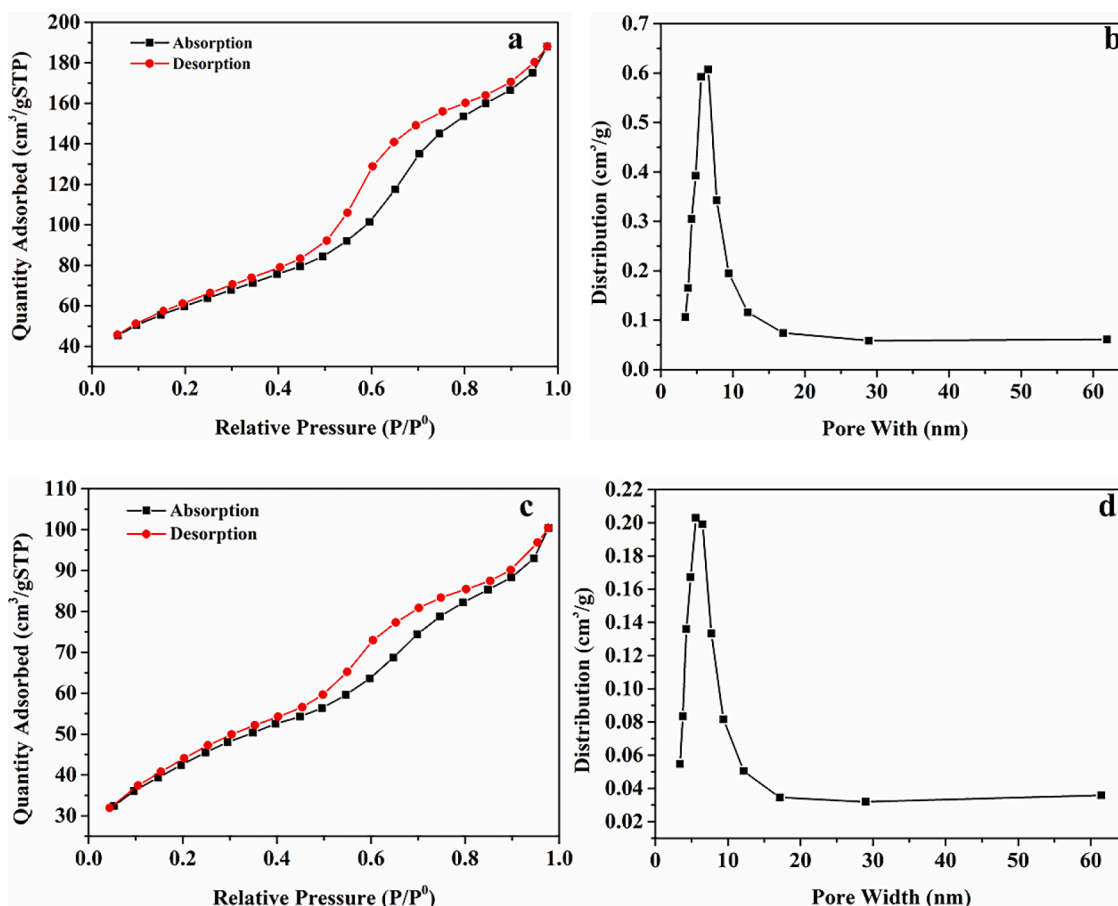


Fig. 4. The specific surface area and pore size distribution of MgO-Al₂O₃ before (a), (b), and after the reaction (c), (d).

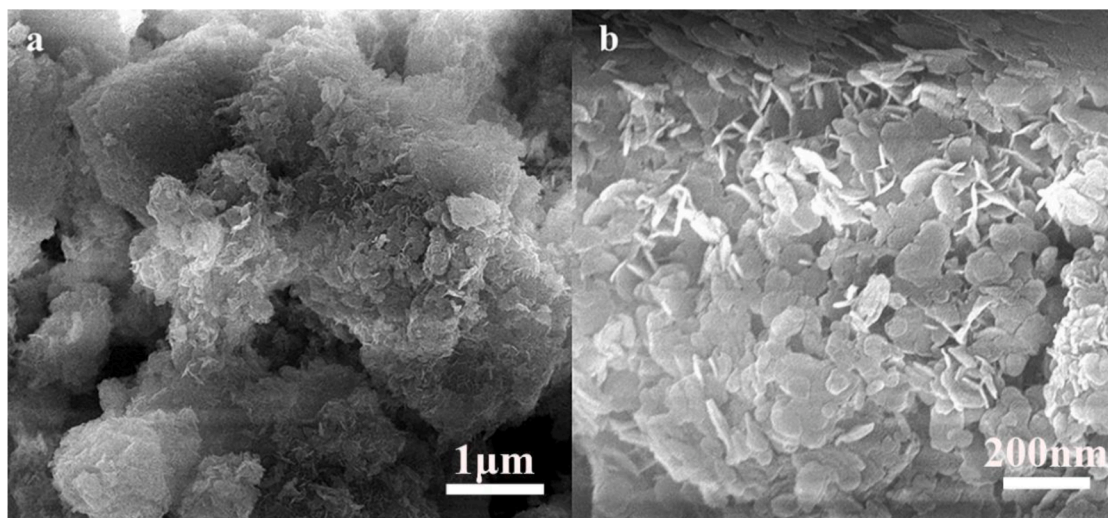


Fig. 5. The SEM of MgO-Al₂O₃.

large difference in the catalytic reaction of FDCA and DMC. Therefore, the chemical state and surface composition of the prepared catalysts were determined using XPS. The O 1s and La 3d_{5/2} nuclear level XPS spectra of the MgO-La₂O₃ sample are shown in Fig. 6c and d, respectively. Three peaks can be identified by deconvolution of the O 1s spectrum (Fig. 6a). The first peak (~528.7 eV) was attributed to the lattice oxygen ion (O²⁻) in metal oxides [26], and the second peak (~531.1 eV) was attributed to hydroxyl and carbonate species. The peak

of 532.6 eV was attributed to the free water adsorbed on the surface [27]. It can be seen in Fig. 6d that the intensity ratio of the main peak to the accompanying peak of La 3d_{5/2} was different at three temperatures, which were 0.63, 0.56 and 0.86, respectively. The intensity ratio represents the magnitude of the force between ligand and La [28]. The lower coordination effect helps to promote the deprotonation of FDCA, which benefits to FDCA methyl esterification.

Fig. 7a showed that the crystal form of MgO-La₂O₃ changed greatly

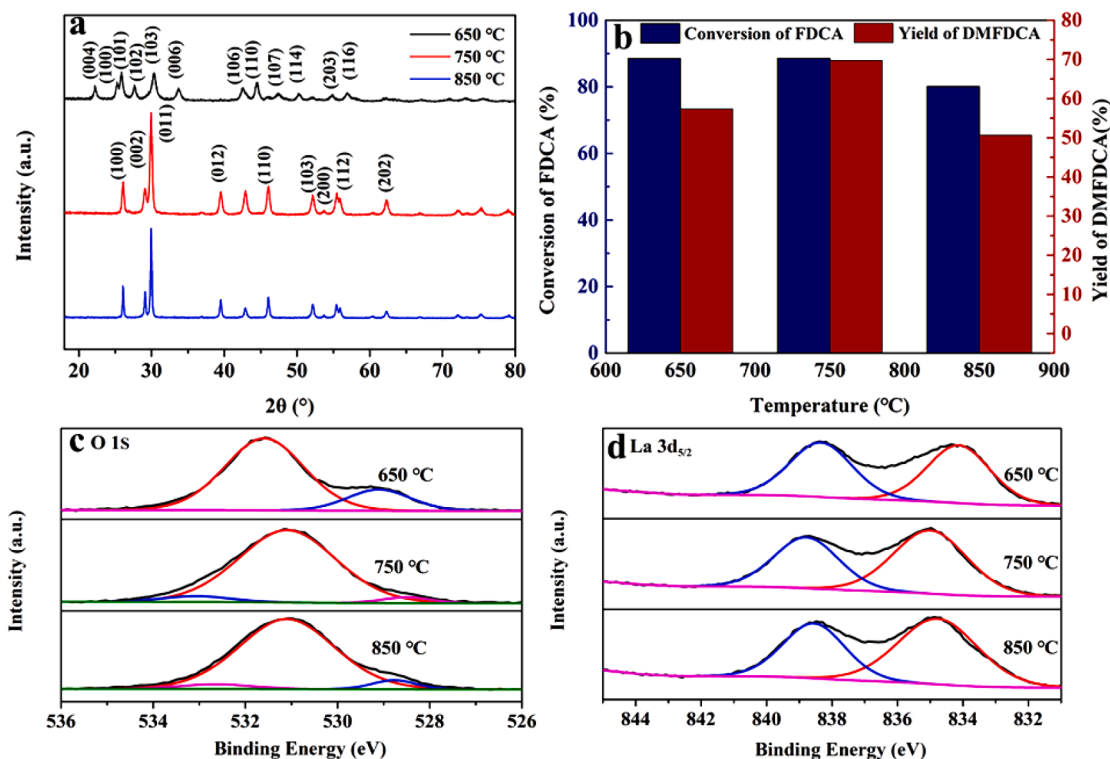


Fig. 6. XRD patterns of (a) Mg-La compounds, (b) Conversion and yield, (c) XPS of O 1 s, and (d) La 3d_{5/2}.

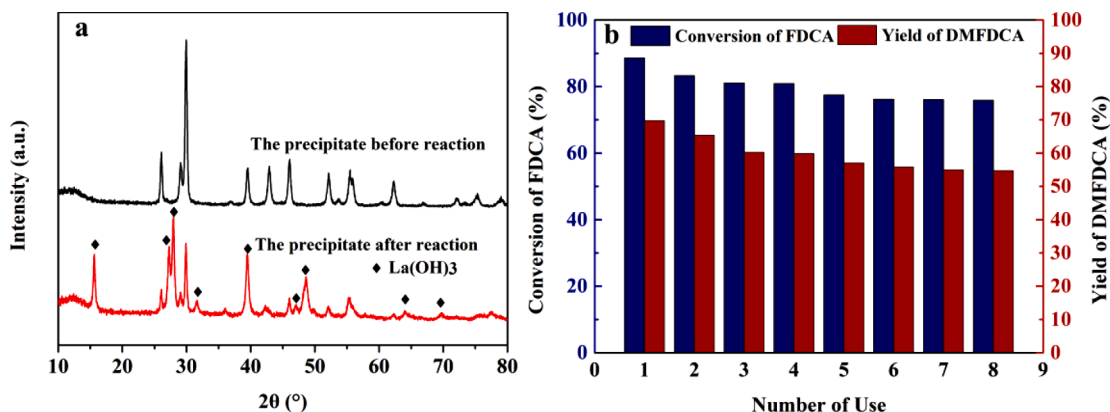


Fig. 7. XRD patterns of MgO-La₂O₃ before and after reaction (a), and the cycle stability of the catalyst (b).

after the reaction, because a portion of La₂O₃ was converted to La(OH)₃ after the reaction. The basicity of La₂O₃ was relatively strong, and its introduction would lead to the decomposition of DMC under high-temperature conditions, resulting in the decline of DMFDCA yield. Meanwhile, La₂O₃ reacted with the generated H₂O to produce La(OH)₃. The yield change in presence of fresh and recycled MgO-La₂O₃ was shown in Fig. 7b. The yield of DMFDCA decreased gradually with the increase of the number of cycling reactions and the generation of La(OH)₃. The alkalinity of La(OH)₃ is stronger than that of La₂O₃, which is more unfavorable for the forward catalytic reaction. Therefore, the conversion of FDCA was 77.47%, and the yield of DMFDCA was 54.99% after 8 recycling reactions.

Another important factor contributing to the decline in catalyst catalytic effectiveness is the decline of the specific surface area and pore size. Fig. 8 shows the N₂ adsorption/desorption isotherm curve of MgO-La₂O₃. The specific surface area of catalysts decreased from 151.4 m²/g to 36.6 m²/g after the reaction, and the pore size distribution also decreased from 15 nm to 5 nm. The adsorption of reactants and products

on the surface of catalysts may be the main reason for the decrease of specific surface area and pore size of catalysts.

Compared with MgO-Al₂O₃, the specific surface area and pore size of MgO-La₂O₃ had more obvious changes, which were mainly caused by the difference in the morphology of the two catalysts. SEM images of MgO-La₂O₃ bimetallic oxides are shown in Fig. 9. MgO-La₂O₃ shows a spindle structure with a rougher surface, which makes it difficult to separate the reactants and products from the catalyst surface at the end of the reaction, thus leading to a lower catalytic effect. The structural and morphological analysis of MgO-La₂O₃ shows that the structural change of the catalyst is also one of the factors affecting the catalytic effect in the reaction system with MgO-La₂O₃ as the catalyst.

3.4. CO₂-TPD

The basicity of the catalyst prepared by hydrothermal method was characterized by CO₂-TPD (up to 750 °C). According to the CO₂-TPD curve, the basicity intensity of the catalyst is distributed in three

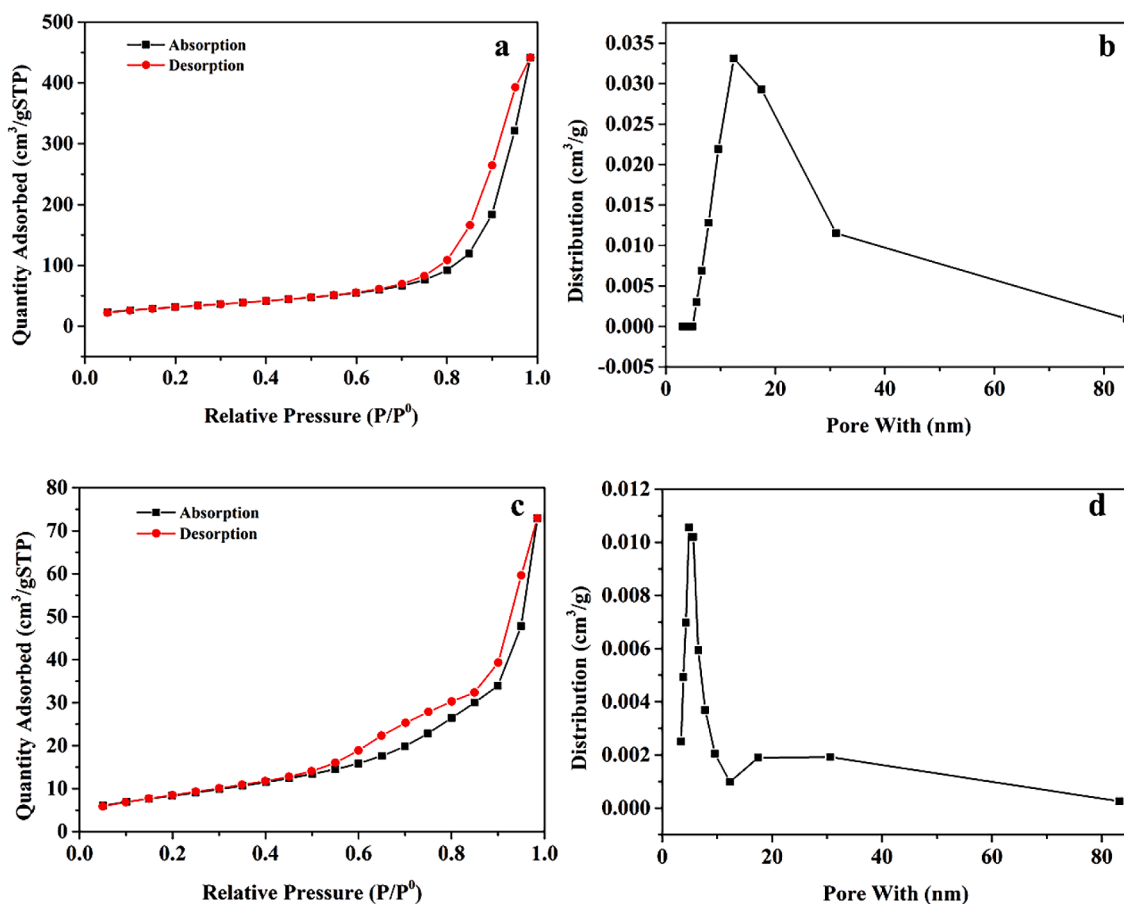


Fig. 8. The specific surface area and pore size distribution of MgO-La₂O₃ before (a), (b), and after the reaction (c), (d).

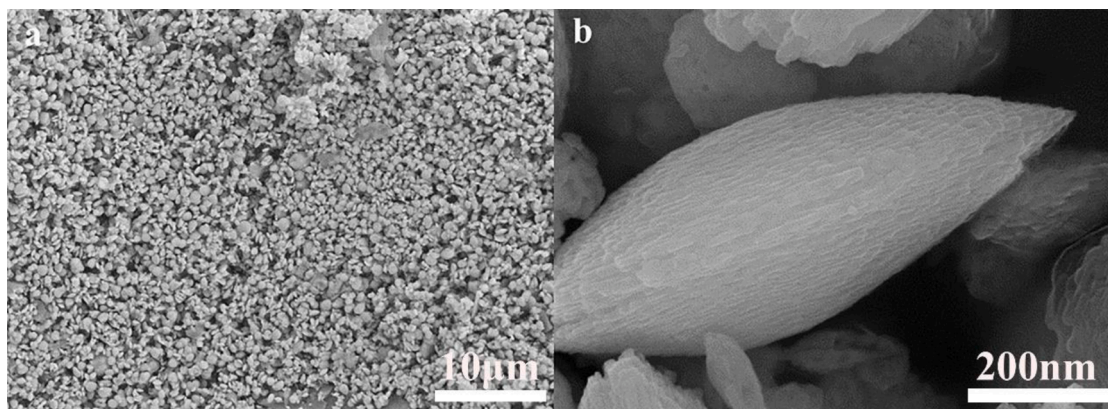


Fig. 9. The SEM of MgO-La₂O₃.

different temperature regions: weak (200–300 °C), medium (300–450 °C) and strong (> 450 °C). In Fig. 10, the CO₂-TPD profile shows the basic strength of MgO-Al₂O₃, MgO-La₂O₃ and MgO [29, 30]. There are obvious differences in the distribution of basic sites in the three catalysts. As shown in Table 2, the basic strength of MgO-La₂O₃ and MgO is mainly medium strong base, and the relative percentage of strong base sites reaches 51.54% and 47.88%, respectively. The presence of Al₂O₃ increases the relative content of weak base in the catalyst, and the relative percentage of weak base in MgO-Al₂O₃ reaches 48.29%. Therefore, MgO-Al₂O₃ is mainly weakly alkaline and moderately alkaline. It can avoid the decomposition of DMC at high temperature in a weakly alkaline environment, and enough base sites can accelerate the

deprotonation of FDCA and the methylation process of DMC.

3.5. Reaction mechanism

The possible esterification mechanism of FDCA with DMC over MgO-Al₂O₃ is shown in Fig. 11. Firstly, FDCA was adsorbed on the basic sites of MgO-Al₂O₃, and then FDCA undergoes deprotonation in the presence of basic sites. Secondly, DMC was adsorbed onto acid sites, and the interaction between acid sites and DMC occurs through the oxygen of the C=O moiety, furthermore an elongation of the O-CH₃ bonds occurs, which justifies the catalytic activity of MgO-Al₂O₃ in esterification reactions [31, 32]. Namely, CH₃⁺ reacted with RCOO⁻ to form the

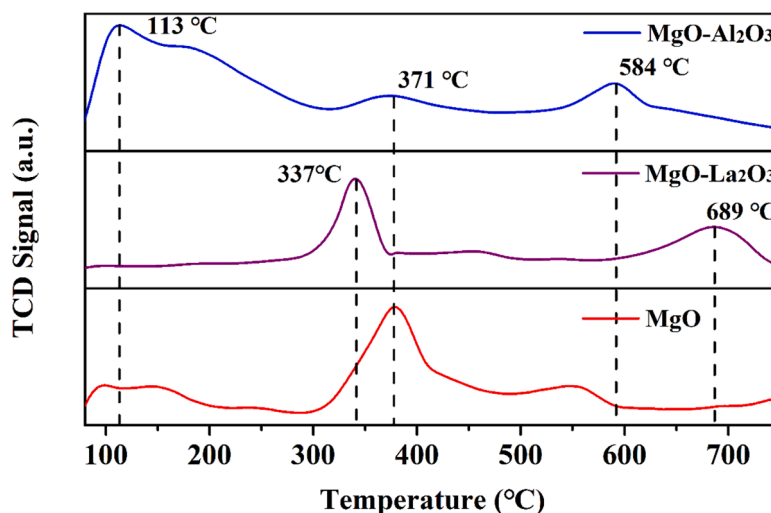


Fig. 10. CO₂-TPD pattern of MgO-Al₂O₃, MgO-La₂O₃, and MgO.

Table 2

The base content profiles of different intensities.

Catalyst	CO ₂ desorption amount (mmol/g)			Total desorption (mmol/g)
	Weak	Moderate	Strong	
MgO-Al ₂ O ₃	0.99 (48.29)	0.48 (23.41)	0.58 (28.29)	2.05
MgO-La ₂ O ₃	0.09 (3.7)	1.09 (44.67)	1.26 (51.64)	2.44
MgO	0.19 (26.76)	0.34 (47.88)	0.18 (25.35)	0.71

The numbers in parentheses indicate the percentage of basic sites of different strengths/%.

esterification product, while H⁺ combines with H₃COCOO⁻ to form CH₃OH and CO₂.

4. Conclusions

In summary, the synergistic effect of metallic oxide and TBAB can effectively catalyze the preparation of DMFDCA from FDCA in DMF. The nucleophilic substitution reaction of S_N2 was greatly facilitated by using MgO-Al₂O₃ as catalyst and DMF as solvent. The metal oxide and TBAB worked cooperatively to improve the DMFDCA selectivity. FDCA was deprotonated on the surface of MgO-Al₂O₃ and TBAB increased the solubility of FDCA in the organic reaction system, resulting in high selectivity to the desired product. This work breaks through the esterification of FDCA by DMC methylation reaction under anhydrous

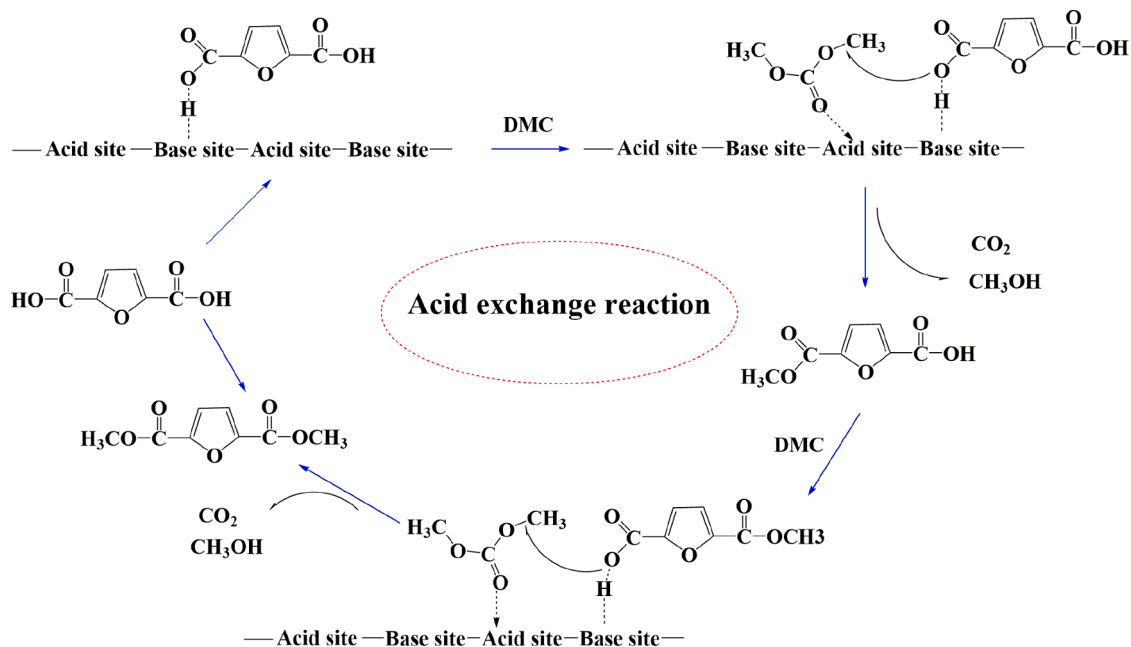


Fig. 11. Reaction mechanism of FDCA and DMC.

conditions, which provides a new, efficient and green route for the preparation of DMFDCA. We think that our reaction system can be used to design other efficient catalytic systems for selective esterification, which is a major advance in green chemistry

Author statement

Chunyu Meng:Data curation, Writing- Original draft preparation.
Kunmei Su:Writing - Review & Editing. **Zhenhuan Li:** Conceptualization. **Maliang Zhang:** Project administration.

Declaration of Competing Interest

The authors declare that they have no known competing financial interests or personal relationships that could have appeared to influence the work reported in this paper.

Acknowledgements

This work was supported by the National Natural Science Foundation of China (no. 21676202 and 21878231), and Natural Science Foundation of Tianjin (no.19JCZDJC37300 and 15JCZDJC37000). This work was also supported by China National Textile and Apparel Council (J201406) and China Petroleum Chemical Co Technology Development Project (218008-6).

References

- [1] I. Delidovich, P.J. Hausoul, L. Deng, R. Pfutzenreuter, M. Rose, R. Palkovits, Alternative monomers based on lignocellulose and their use for polymer production, *Chem. Rev.* 116 (2016) 1540–1599.
- [2] A. Gandini, T.M. Lacerda, From monomers to polymers from renewable resources: recent advances, *Prog. Polym. Sci.* 48 (2015) 1–39.
- [3] N. Hernandez, R.C. Williams, E.W. Cochran, The battle for the "green" polymer. different approaches for biopolymer synthesis: bioadvantaged vs bioreplacement, *Org. Biomol. Chem.* 12 (2014) 2834–2849.
- [4] Z. Zhang, K. Deng, Recent advances in the catalytic synthesis of 2,5-furandicarboxylic acid and its derivatives, *ACS. Catal.* 5 (2015) 6529–6544.
- [5] A. Lolli, S. Albonetti, L. Utili, R. Amadori, F. Ospitali, C. Lucarelli, F. Cavani, Insights into the reaction mechanism for 5-hydroxymethylfurfural oxidation to FDCA on bimetallic Pd–Au nanoparticles, *Appl. Catal. A: Gen.* 504 (2015) 408–419.
- [6] W.W. Ali Hussain Motagamwala, Canan Sener, David Martin Alonso, Christos T. Maravelias, James A. Dumesic, Toward biomass-derived renewable plastics: production of 2,5-furandicarboxylic acid from fructose, *Sci. Adv.* 4 (2018).
- [7] C.S. López-Garzón, L.A. Wielen, A.J.J. Straathof, Ester production from bio-based dicarboxylates via direct downstream catalysis: succinate and 2,5-furandicarboxylate dimethyl esters, *RSC. Adv.* 6 (2016) 3823–3829.
- [8] Y. Yang, Y. Wang, S. Li, X. Shen, B. Chen, H. Liu, B. Han, Selective hydrogenation of aromatic furfurals into aliphatic tetrahydrofurfural derivatives, *Green. Chem.* 22 (2020) 4937–4942.
- [9] G.Z. Papageorgiou, D.G. Papageorgiou, Z. Terzopoulou, D.N. Bikiaris, Production of bio-based 2,5-furan dicarboxylate polyesters: recent progress and critical aspects in their synthesis and thermal properties, *Eur. Polym. J.* 83 (2016) 202–229.
- [10] A. Cho, S. Byun, J.H. Cho, B.M. Kim, AuPd-Fe₃O₄ nanoparticle-catalyzed synthesis of Furan-2,5-dimethylcarboxylate from 5-hydroxymethylfurfural under mild conditions, *ChemSusChem* 12 (2019) 2310–2317.
- [11] L. Diao, K. Su, Z. Li, C. Ding, Furan-based co-polyesters with enhanced thermal properties: poly(1,4-butylene-co-1,4-cyclohexanedimethylene-2,5-furandicarboxylic acid), *RSC. Adv.* 6 (2016) 27632–27639.
- [12] S. Thiyagarajan, W. Vogelzang, R.J.I. Knoop, A.E. Frissen, J. Havenen, D.S. Es, Biobased furandicarboxylic acids (FDCA): effects of isomeric substitution on polyester synthesis and properties, *Green. Chem.* 16 (2014) 1957–1966.
- [13] S. Liu, X. Fu, J. Dai, Z. Liu, L. Zhu, C. Hu, One-Pot synthesis of 2,5-diformylfuran from fructose by bifunctional polyaniline-supported heteropolyacid hybrid catalysts, *Catalysts* 9 (2019) 134–140.
- [14] R. Sharath, N. Murthyb, Esterification of salicylic acid over zeolites using dimethyl carbonate, *Appl. Catal. A: Gen.* 226 (2002) 175–182.
- [15] P. Tundo, M. Selva, The chemistry of dimethyl carbonate, *Acc. Chem. Res.* 35 (2002) 706–716.
- [16] P. Tundo, M. Musolino, F. Aricò, The reactions of dimethyl carbonate and its derivatives, *Green. Chem.* 20 (2018) 28–85.
- [17] P. Tundo, M. Selva, J. Perosa, Reaction of functionalized anilines with dimethyl carbonate over NaY faujasite chemoselectivity toward mono-N-methylation, *Org. Chem.* 68 (2003) 7374–7378.
- [18] L. Desidery, N. Chaemcheun, M. Yusubov, F. Verpoort, Di-methyl carbonate transesterification with EtOH over MOFs: basicity and synergic effect of basic and acid active sites, *Catal. Commun.* 104 (2018) 82–85.
- [19] J. Shi, G. Liu, Z. Fan, L. Nie, Z. Zhang, W. Zhang, Q. Huo, W. Yan, M. Jia, Amorphous mesoporous aluminophosphate as highly efficient heterogeneous catalysts for transesterification of diethyl carbonate with dimethyl carbonate, *Catal. Commun.* 12 (2011) 721–725.
- [20] K. Gupta, R.K. Rai, S.K. Singh, Metal catalysts for the efficient transformation of biomass-derived HMF and furfural to value added chemicals, *ChemCatChem* 10 (2018) 2326–2349.
- [21] H. Hattori, Solid base catalysts: generation of basic sites and application to organic synthesis, *Appl. Catal. A: Gen.* 222 (2001) 247–259.
- [22] A. Shaheen, S. Sultana, H. Lu, M. Ahmad, M. Asma, T. Mhmoed, Assessing the potential of different nano-composite (MgO, Al₂O₃-CaO and TiO₂) for efficient conversion of silybum eburneum seed oil to liquid biodiesel, *J. Mol. Liq.* 249 (2018) 511–521.
- [23] H.X.Li Y.Wang, X.G. Li, D. Chen, W.D. Xiao, Effective iron catalysts supported on mixed MgO–Al₂O₃ for Fischer–Tropsch synthesis to olefins, *Ind. Eng. Chem. Res.* 59 (2020) 11462–11474.
- [24] M. Liu, S. Zanna, H. Ardelean, I. Frateur, P. Schmutz, G. Song, A. Atrens, P. Marcus, A first quantitative XPS study of the surface films formed, by exposure to water, on Mg and on the Mg–Al intermetallics: al₃Mg₂ and Mg₁₇Al₁₂, *Corros. Sci.* 51 (2009) 1115–1127.
- [25] F. Wang, N. Ta, Y. Li, W. Shen, La(OH)₃ and La₂O₂CO₃ nanorod catalysts for claisen-schmidt condensation, *Chin. J. Catal.* 35 (2014) 437–443.
- [26] M.M. Natile, A. Galenda, A. Glisenti, From La₂O₃ to LaCoO₃: XPS analysis, *Surf. Sci. Spectra* 15 (2008) 1–13.
- [27] K. Suththumporn, S. Kawi, Promotional effect of alkaline earth over Ni–La₂O₃ catalyst for CO₂ reforming of CH₄: role of surface oxygen species on H₂ production and carbon suppression, *Int. J. Hydrogen Energy* 36 (2011) 14435–14446.
- [28] X. Dong, Y. Jiang, W. Shan, M. Zhang, A novel highly ordered mesoporous carbon-based solid acid for synthesis of bisphenol-A, *Rsc Adv.* 6 (2016) 17118–17124.
- [29] J. Molleti, G.D. Yadav, Potassium modified La-Mg mixed oxide as active and selective catalyst for mono-methylation of phenylacetone nitrile with dimethyl carbonate, *Mol. Catal.* 438 (2017) 66–75.
- [30] Q. Zhou, H. Zhang, F. Chang, H. Li, H. Pan, W. Xue, D.-Y. Hu, S. Yang, Nano La₂O₃ as a heterogeneous catalyst for biodiesel synthesis by transesterification of *Jatropha curcas* L. oil, *J. Ind. Eng. Chem.* 31 (2015) 385–392.
- [31] Y. Gao, Z. Li, K. Su, B. Cheng, Excellent performance of TiO₂(B) nanotubes in selective transesterification of DMC with phenol derivatives, *Chem. Eng. J.* 301 (2016) 12–18.
- [32] K. Su, Z. Li, B. Cheng, K. Liao, D. Shen, Y. Wang, Studies on the carboxymethylation and methylation of bisphenol A with dimethyl carbonate over TiO₂/SBA-15, *J. Mol. Catal. A: Chem.* 315 (2010) 60–68.